Thermochromic Polydiacetylene Micro- and Nanocrystals: An Unusual Size Effect in Electronic Spectra

Xiaoyu Wang and Daniel J. Sandman*

Center for Advanced Materials, Department of Chemistry, University of Massachusetts Lowell, Lowell, Massachusetts 01854-5046

Shujun Chen and Samuel P. Gido*

Department of Polymer Science and Engineering, University of Massachusetts Amherst, Amherst, Massachusetts 01003

Received April 6, 2007; Revised Manuscript Received November 19, 2007

ABSTRACT: Micro- and nanoscale crystals of the thermochromic polydiacetylenes (PDAs) ETCD and PUDO exhibit electronic absorption maxima at wavelengths longer than those observed in bulk crystal specimens of the same materials. This observation is in contrast to the reported behavior of PDA−DCH where the absorption maximum shifts to shorter wavelengths as crystal size decreases. Infrared spectra and X-ray powder data indicate that the small crystals have the same composition and a structure similar to the bulk specimens. Differential scanning calorimetry (DSC) reveals a larger endothermic heat of the thermochromic phase transition in the small crystals vs bulk specimens. The crystal morphology and structure of microsized, nanosized, and bulk crystals of PDA−ETCD and PDA−PUDO were studied by transmission electron microscopy (TEM) and electron diffraction (ED). For both PDAs, no drastic changes in lattice parameters were observed as crystal size decreases from bulk to micro- and nanoscale.

Introduction

The preparation and characterization of polydiacetylene (PDA) micro- and nanosized crystals by the reprecipitation method[1] have allowed the study of PDAs and their properties in a new morphology. The reprecipitation method involves pouring a diacetylene (DA) monomer solution into a poor solvent, usually water, under vigorous stirring. This is typically followed by polymerization initiated by ultraviolet light. The crystals thus formed have good dispersion for long periods of time (several days to several months). Micro- and nanosized PDA crystals prepared by this method were found to be of interest for the assessment of third-order[2] and fifth-order[3] nonlinear optical properties of the PDA of 1,6-di-*N*-carbazolyl-2,4-hexadiyne (DCH, **1a**). Diacetylene polymerization and the molecular structures of PDAs under discussion are illustrated in Figure 1.

A noteworthy property of micro- and nanocrystals of PDA−DCH is the shift to shorter wavelengths of the wavelength of strongest visible absorption as crystal size decreases from bulk to nanoscale.[4] In earlier work, we have reproduced this spectral behavior and also prepared an electrostatic assembled film of PDA−DCH nanocrystals and poly(diallyldimethylammonium chloride).[5] These films were exposed to liquid bromine under conditions[6] that convert PDA−DCH to a mixed polyacetylene structure. These brominated films allowed observation of the visible spectrum of brominated PDA−DCH[5,6] with maxima at 540 and 479 nm. These features were not observed in diffuse reflectance of brominated PDA−DCH.[7]

In connection with our interest in the possibility that the thermochromic phase transition in the PDA of *bis*-alkylurethanes of 5,7-dodecadiyn-1,12-diol involved an aggregate structure of several chains in contrast to the need for only a single chain,[8] we prepared micro- and nanoscale crystals of the monomers of the *bis*-ethyl (**1b**, ETCD) and *bis*-*n*-propyl (**1c**, PUDO) urethanes by the reprecipitation method followed by ultrasonic irradiation (42 kHz). We then polymerized them with 254 nm UV light. This preparative work has been previously described.[9] These reduced-sized PDA specimens are found to exhibit the thermochromic phase transition at the usual temperatures. We now describe the optical properties of these crystals and our characterization of them. In addition, transmission electron microscopy (TEM) and electron diffraction (ED) were used to study the morphology of PDA crystals of various sizes and to attempt identification of possible structural changes associated with the reduction in crystal size. We note that other ultrasmall crystals of these PDA prepared[9] by methods other than the reprecipitation work described herein do not have the optical properties described herein for crystals prepared by reprecipitation.

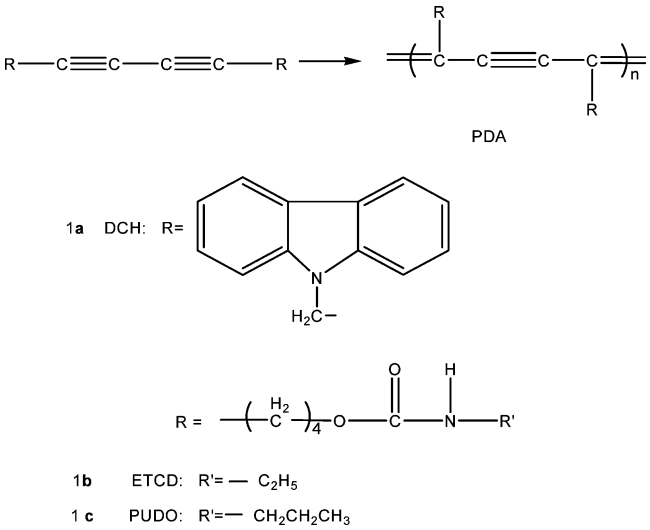

Figure 1. Diacetylene polymerization and repeat structures and abbreviations for PDAs under discussion.

10.1021/ma070820x CCC: $40.75
Published on Web 01/16/2008

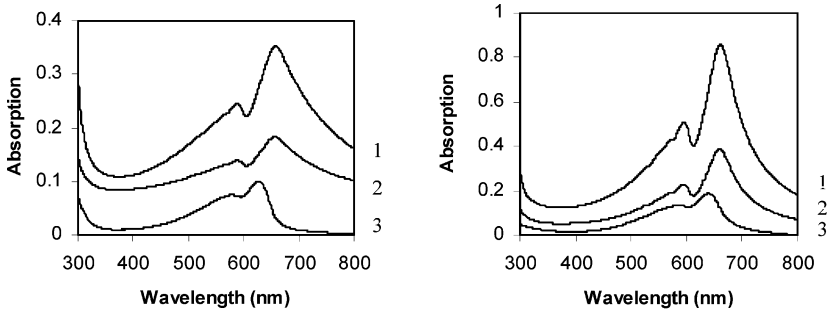

Figure 2. Electronic absorption spectra: (a) 1 (1−2 μm), 2 (∼250 nm), and 3 (bulk) are PDA−ETCD micro-, nano-, and bulk crystals, respectively. (b) 1 (∼1 μm), 2 (∼350 nm), and 3 (bulk) are PDA−PUDO micro-, nano-, and bulk crystals, respectively.

Table 1. X-ray Powder Diffraction Data

PDA	size of PDA crystals	2θ, deg	*d*-spacings, nm
ETCD	bulk	4.8, 9.6, 14.3	18.4, 9.2, 6.19
ETCD	∼1 μm	4.8, 9.7, 14.6	18.4, 9.1, 6.06
ETCD	∼350 nm	4.8, 9.7, 14.6	18.4, 9.1, 6.06
PUDO	bulk	4.3, 8.8, 13.2	20.1, 10.1, 6.68
PUDO	∼1 μm	4.3, 8.8, 13.2	20.1, 10.1, 6.68
PUDO	∼300 nm	4.3, 8.8, 13.2	20.1, 10.1, 6.68

Experimental Section

Diacetylene monomers were synthesized as previously[10] described. Micro- and nanoscale crystals were prepared as reported[9] earlier. Ultraviolet irradiation with 254 nm light was carried out with Osram-Sylvania herbicidal lamps. Visible spectra were recorded on a UV/vis/NIR spectrometer (Perkin-Elmer Lambda 9) using 1 cm cells. Differential scanning calorimetry (DSC) was carried out on a TA Thermal Analysis System Q100 to measure the thermochromic transition temperature and heat of the transition.

Samples for TEM and ED were prepared by drop-casting the respective PDA crystal−water dispersions onto carbon-coated copper grids, which were then allowed to air-dry at room temperature overnight. A JEOL 2000FX transmission electron microscope was used to characterize the morphology of PDA−ETCD and PDA−PUDO bulk, microscale, and nanoscale crystals and the corresponding electron diffraction patterns at 200 kV accelerating voltage. Analysis of the beam stability of these PDA micro- and nanocrystals indicated an end-point dose of $J_e \approx 0.38$ C cm^{-2} at 200 kV, which is comparable to what was reported for PDA−DCH nanocrystals.[11] In performing TEM and ED experiments, care was taken to limit unnecessary electron beam exposure, thus minimizing electron beam damage and producing the best possible electron diffraction patterns. This included such standard procedures as focusing on an adjacent area to the area where data were recorded, using the smallest possible spot size, limiting the spread of the beam, and turning the beam off when it was not needed. Also, the ED data were recorded on fast X-ray film (Kodak DEF5) rather than standard EM film for faster acquisition. Typical conditions for acquiring ED patterns were a magnification of 25 000×, beam intensities of 4−5 pA cm^{-2}, and exposure times of 4−8 s. Therefore, the total dose used to obtain the ED patterns was limited to 0.01−0.025 C cm^{-2}, well below the end-point dose.

Results and Discussion

PDA−ETCD and PDA−PUDO microsized (1−2 μm in length) and nanosized (250−350 nm) crystals exhibited absorption spectra with maxima at 655 and 660 nm, respectively, when suspended in water at room temperature. In this work when we describe crystals as having a certain length, the cited length is an average.[9] For example, using an ETCD solution 5×10^{-3} M, the average length of PDA−ETCD crystals is 370 nm with a size range from 150 to 770 nm. These spectra exhibit vibronic structure and are shown in Figure 2. These PDA crystals were prepared using 254 nm UV light for an irradiation period of 20 min. The spectra in Figure 2 did not change with longer periods of UV irradiation. These maxima are to be compared to those reported for bulk crystals of PDA−ETCD[12] and PDA−PUDO,[13] 635 and 640 nm, respectively. This amounts to a shift to lower energy of about 0.06 eV between spectral maxima in bulk crystals and microcrystals. Hence, in contrast to PDA−DCH, where the absorption maximum shifts to shorter wavelength as crystal size decreases, in these thermochromic PDA specimens the absorption maximum shifts to longer wavelengths as crystal size decreases from bulk crystals to those with micron or smaller dimensions. We now seek to identify possible differences between bulk PDA crystals and the micron and smaller size crystals.

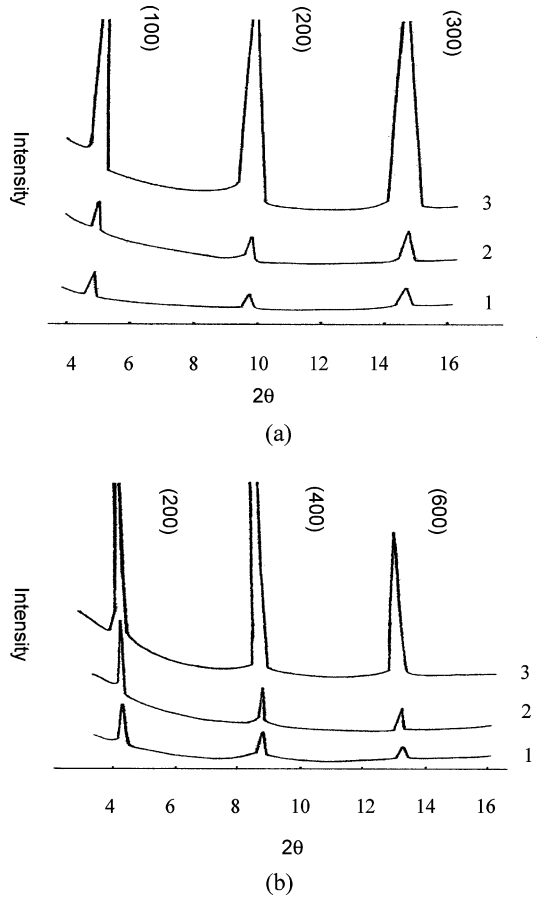

Figure 3. X-ray powder diffraction patterns of (a) 1, 2, and 3 are PDA−ETCD nano-, micro-, and bulk crystals. (b) 1, 2, and 3 are PDA−PUDO nano-, micro-, and bulk crystals, respectively. The *h*00 reflections are indicated.

FTIR spectra of the micro- and nanoscale PDA specimens are indistinguishable from those of the bulk specimens. Hence,

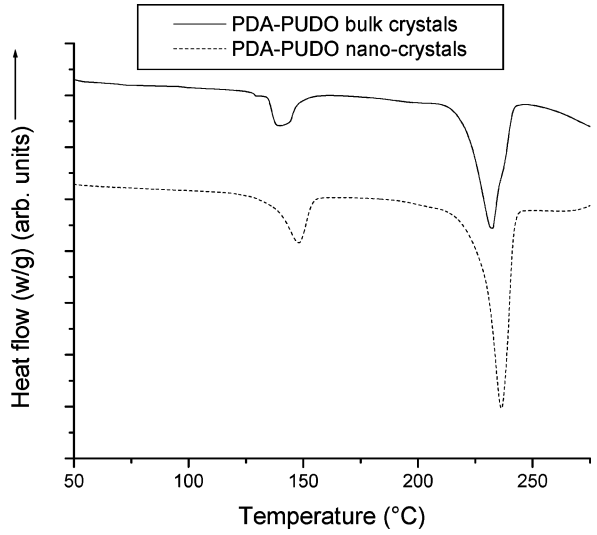

Figure 4. DSC scans of PDA−PUDO bulk and nanocrystals.

Table 2. DSC of PDA−PUDO

sample size	thermochromic transition temp, °C	heat of the transition, J/g
bulk	136.2	19.10
bulk	136.3	19.99
300−400 nm	136.9	23.33
300−400 nm	136.4	23.27
300−400 nm (2nd heating)	135.3	15.20

there is no compositional difference between the two kinds of materials. X-ray powder diffraction was recorded at room temperature for bulk, microscale, and nanoscale crystals of PDA−ETCD and PDA−PUDO. The data are summarized in Table 1. The low-angle ($2\theta = 4-20°$) diffraction of both PDAs is dominated by the *h*00 reflections, and the three specimens of each PDA have similar diffraction patterns. These are in accord with literature[14] data and indicate that the micro- and nanoscale crystals have a structure similar to the bulk crystals. X-ray diffraction patterns of these crystals are shown in Figure 3.

If the average crystal size in a powder specimen is below a certain limit, broadening of diffracted X-rays may occur. Further, crystals under mechanical strain may exhibit shifts in *d*-spacings or additional broadening.[15] We have not seen such indications in our X-ray data.

Differential Scanning Calorimetry of PDA−PUDO. Differential scanning calorimetry (DSC) has revealed a difference between nanoscale and bulk crystals of PDA−PUDO. The data that we have acquired are summarized in Table 2, and DSC scans of bulk and nanocrystals are compared in Figure 4. The data summarized in Table 2 are taken from individual experiments on different specimens. The thermochromic phase transition temperature of both bulk and nanocrystals is in agreement with a previous[16] report. However, the heat associated with the transition is greater in the nanocrystals than in the bulk specimens by about 16%. Further, when a nanocrystal specimen is heated to 180 °C, cooled to room temperature, and reheated, the phase transition temperature decreases by about 1 °C and the heat of the transition decreases by about 1/3. The decrease in phase transition temperature on second heating in the nanocrystals is analogous to what was observed in PDA−IPUDO.[17] In Figure 4, the feature near 225 °C is the melting point of the polymer.

We suggest that the shift of the absorption maximum to longer wavelengths in micro- and nanocrystals compared to bulk specimens is associated with an increase in mechanical strains

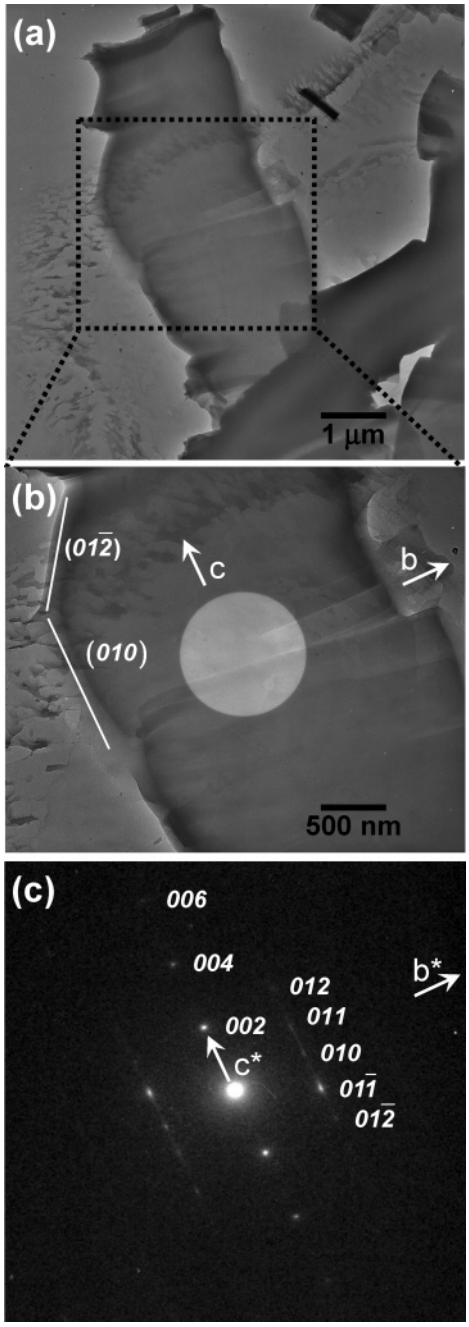

Figure 5. (a) TEM image of a representative bulk PDA−ETCD crystal. (b) Higher magnification image of the boxed area in (a), where the *b* and *c* crystal axes are labeled as white arrows and two distinctive crystal facets highlighted with white lines. (c) ED pattern taken from the center of the crystal in (b), as indicated by the selected area aperture or the lighter contrast circled area. The relative orientations of the crystal to the ED pattern are preserved in (a)−(c). (c) is a typical ED pattern from zone [100], where the reciprocal crystal axes *b** and *c** and major 0*kl* reflections are labeled.

on the conjugated backbone. If one builds a molecular model of these thermochromic PDA, one observes that the four methylene groups are in a strained gauche conformation. We assume that the population of such conformations is increased in the micro- and nanocrystals relative to the bulk specimens. It is likely that, as the material is heated above the thermochromic phase transition, the side-group conformation population tends toward the lower energy staggered conformation. The heat associated with the transition is larger in the nanocrystals as more high energy conformations change toward the lower energy form in these crystals.

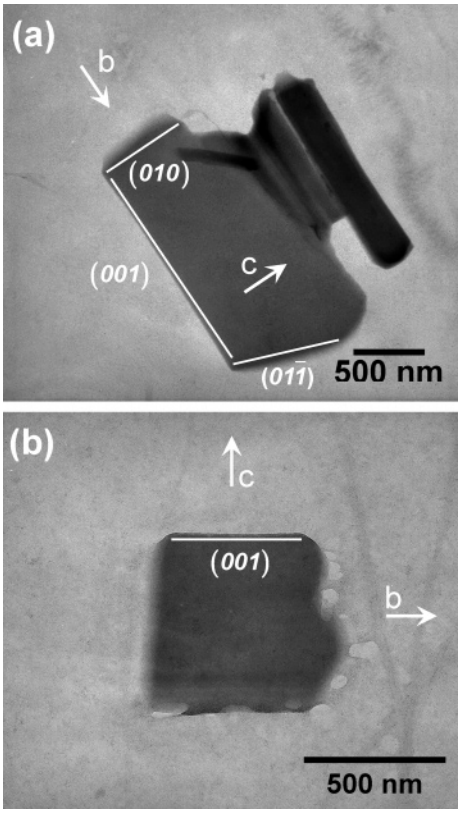

Figure 6. (a) TEM image of a representative PDA−ETCD microcrystal. (b) TEM image of a representative PDA−ETCD nanocrystal. In both images, the crystal axes and distinctive crystal facets are labeled with white arrows and white lines.

Transmission Electron Microscopy and Electron Diffraction. PDA−ETCD and PDA−PUDO crystals of three different sizes shown in Table 1 were previously[9] studied by scanning electron microscopy (SEM) and here studied by transmission electron microscopy (TEM) and electron diffraction (ED). SEM images of PDA−PUDO[9] revealed a mixture of needles, prisms, and more complex crystalline forms. Examination of the needles under polarized optical microscopy revealed growth along the *b*-axis.

PDA−ETCD. Figure 5a shows the TEM micrograph of a bulk crystal of PDA−ETCD, whereas Figure 5b is a higher magnification TEM image of the boxed area in Figure 5a. Figure 5c is the ED pattern taken from the center of the crystal in Figure 5b, as indicated by the selected area aperture or the lighter contrast circled area. The relative orientations of the crystal to the ED pattern are preserved in these figures. Therefore, the *b* and *c* crystal axes can be determined on the basis of the corresponding *b**- and *c**-axes, as demonstrated in Figure 5b. Note that the unit cell of PDA−ETCD bulk crystal is monoclinic,[12] with $\beta = 95°$; thus, *b* is parallel to *b**, while the actual *c*-axis is pointing slightly inward with respect to the image plane. The drawn *c*-axis is therefore the projection of the actual *c*-axis onto the image plane. The crystal facets in Figure 5b are found to be those of (010) and (01$\bar{2}$), whereas the cracks are parallel to the *b*-axis, i.e., the chain axis, as would be expected for typical PDA crystals. Figure 5a,b reveals crystal growth along the *b*-axis for the bulk crystal, consistent with the polarized optical microscopy results. The ED pattern in Figure 5c is a typical ED pattern of bulk PDA−ETCD crystal, from zone [100], or *b**−*c** plane, where only 0*kl* reflections are observed. The predominating observation of zone [100] ED patterns can be attributed to the preferential orientation of the *a*-axis of the PDA crystal, which is along its thickness direction and parallel to the electron beam when performing electron diffraction on these PDA crystals.

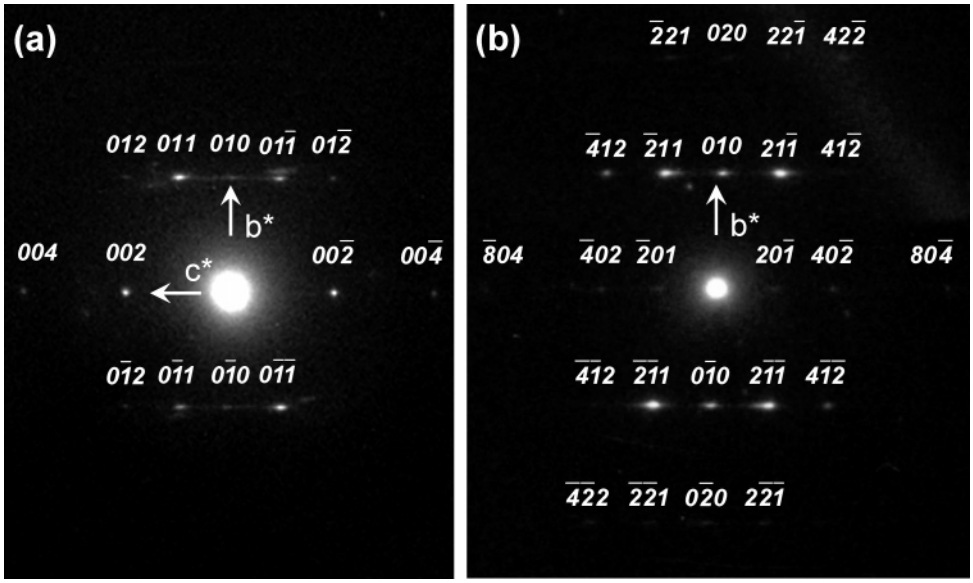

Figure 7. (a) A typical ED pattern from zone [100] of PDA−PUDO bulk crystal, with *b**- and *c**-axes and all observed 0*kl* reflections labeled. (b) ED pattern from zone [102] of a PDA−PUDO bulk crystal, with *b**-axis and all observed reflections labeled.

Table 3. Lattice Parameters for PDA−ETCD and PDA−PUDO Crystals of Various Sizes

	PDA−ETCD single crystal			PDA−PUDO single crystal		
lattice parameter, Å	bulk	micro	nano	bulk	micro	nano
a				41.25 ± 0.28	40.39 ± 0.56	
b	4.78 ± 0.06	4.81 ± 0.06	4.81 ± 0.06	4.81 ± 0.06	4.76 ± 0.06	4.83 ± 0.06
c	10.55 ± 0.07	10.47 ± 0.14	10.48 ± 0.07	10.76 ± 0.07	10.48 ± 0.14	10.68 ± 0.05

Representative PDA−ETCD micro- and nanocrystals are shown in parts a and b of Figure 6, respectively, with their *b* and *c* crystal axes and crystal facets labeled. As PDA−ETCD bulk crystals, the PDA−ETCD micro- and nanocrystals also have crystal growth along the *b*-axis. For all PDA−ETCD crystals shown in Figures 5 and 6, the (010) facets are not as sharp or well-defined as the (001) facets, which may be attributed to the high concentration of chain ends on (010) facets and the hydrogen-bonded sheets on the (001) facets. In addition to the two main crystal facets, nonorthogonal facets such as (011) and (012) are also found in these crystals, as seen in Figures 5b and 6a. The electron diffraction patterns from the PDA−ETCD micro- and nanocrystals (not shown) are similar to that of the bulk crystal as seen in Figure 5c. On the basis of the zone [100] electron diffraction data, the *b* and *c* lattice parameters can therefore be extracted for various sized PDA−ETCD crystals. The extracted *b* and *c* lattice parameters for bulk, microsized, and nanosized PDA−ETCD crystals are listed in Table 3. Our data for bulk PDA−ETCD crystal are in good agreement with those from previous reports of blue phase bulk PDA-ETCD single crystals.[14a,b]

The presence of streaks in the ED pattern of PDA−ETCD (Figure 5c) and PDA−PUDO is not surprising. Streaks were observed in the single-crystal X-ray photographs of PDA−ETCD,[14a] and they are present due to disorder that arises from a lattice mismatch between the growing polymer chains in the monomer lattice.

PDA−PUDO. In the case of PDA−PUDO bulk crystal, electron diffraction patterns from more than one zone were obtained, which allowed us to extract all three lattice parameters (*a*, *b*, and *c*). In Figure 7a, a typical ED pattern from zone [100] for PDA−PUDO bulk crystal is shown, with all observed 0*kl* reflections labeled. Because of the presence of streaks along the layer lines parallel to *c**-axis, the observed maxima for 010 and $0\bar{1}0$ are slightly off *b**-axis. Similar off *b**-axis maxima were seen in a previously reported ED pattern of PDA−ETCD single crystals from the same zone.[14b] Figure 7b shows the ED pattern from a different zone, zone [102] for a PDA−PUDO bulk crystal. The measured *d*-spacings from this pattern agree well with those calculated on the basis of the orthorhombic unit cell for PDA−PUDO single crystal reported by Koshihara et al.,[14c] obtained from X-ray diffraction. Earlier, imaging of three different crystal zones and their corresponding fast Fourier transformation (FFT) patterns were reported[11] for PDA−DCH. To the best of our knowledge, there have been no previous reports on electron diffraction patterns from multiple zones for thermochromic PDA single crystals.

Likewise for PDA−PUDO microcrystal, all three lattice parameters were obtained from electron diffraction data from zones [100] and [001]. For PDA−PUDO nanocrystal, ED patterns from only zone [100] were acquired, which allowed us to extract *b* and *c* lattice parameters. A representative PDA−PUDO nanocrystal is seen in Figure 8a, while the corresponding ED pattern from this crystal is shown in Figure 8b, where well-preserved reflections up to the fourth layer line (04*l* reflections) parallel to *c** are obtained.

The crystal lattice parameters for the bulk, microsized, and nanosized crystals of PDA−ETCD and PDA−PUDO are summarized in Table 3. It is clear from Table 3 that for both PDAs the crystal lattice parameters do not show drastic changes when the crystal size decreases from bulk to micro- and nanoscales.

It is our assumption that the shift to longer wavelength of the spectra of the micro- and nanosized PDA crystals involves

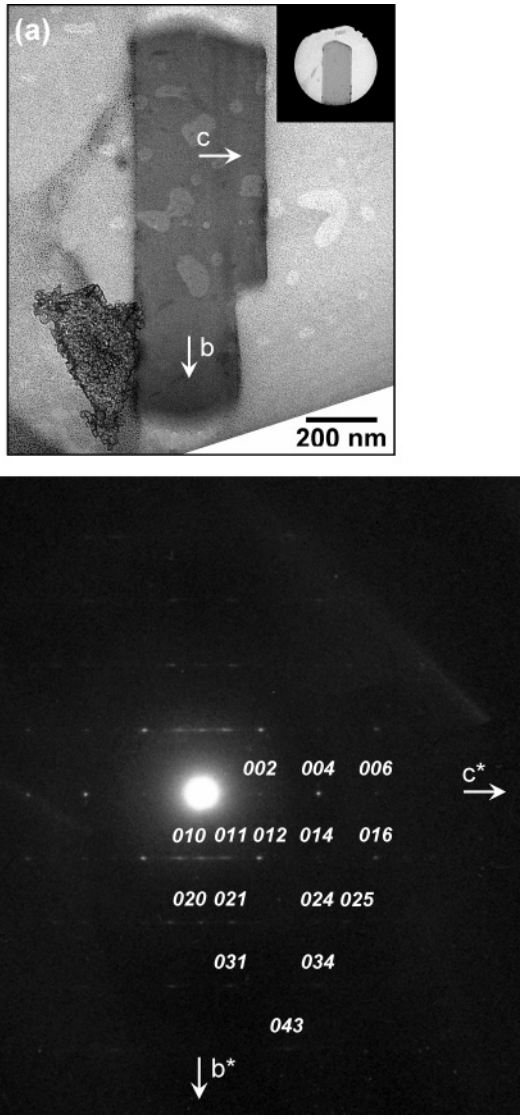

Figure 8. (a) TEM image of a representative PDA−PUDO nanocrystal, with its *b* and *c* crystal axes labeled. The inset is a defocused image of (b), revealing the area taken for electron diffraction is the top part of the nanocrystal. (b) Corresponding ED pattern for the nanocrystal in (a), from zone [100], showing well-preserved reflections up to the fourth layer line (04*l* reflections) parallel to *c**-axis. The *b**- and *c**-axes and major reflections are labeled.

a modest enhancement of the mechanical strains likely present in the bulk crystals. We have earlier reported[18] solid-state NMR data that support the involvement of mechanical strains in the thermochromic phase transition of these PDA, namely that mechanical strains on the PDA backbone at ambient temperature are partially relieved on heating above the temperature of the thermochromic phase transition. The shift of the spectrum associated with thermochromism of these PDAs is ∼0.35 eV and involves a volume expansion of the crystallographic unit cell of 2.5−3.0%.[14c] As noted above, the shift in the electronic spectrum between bulk crystals and the smaller crystals is about 0.06 eV. If the unit cell volume scales with the energy magnitude of the spectral shift, the volume change between bulk crystal and the smaller crystals would be about 0.5%. With reference to Table 3 and the literature,[14c] the range of unit cell volumes is significantly greater than 0.5%. Hence, it is likely that any change in unit cell dimensions as a result of increased mechanical strains may not be readily detectable under the present conditions.

Conclusion

Micro- and nanosized PDA−ETCD and PDA−PUDO crystals were successfully fabricated, and their shapes are those of rectangular prisms. Red-shifting occurs after PDA−ETCD and PDA−PUDO crystals are decreased to micro- and nanoscale, and these phenomena are related to the stress on the main chains. The preparation of PDA−ETCD and PDA−PUDO crystals on micro- and nanoscale results in higher stress on the crystal main chains, which causes longer wavelength absorption. By comparing the crystal lattice parameters of PDA−ETCD and PDA−PUDO bulk crystals with those of their corresponding micro- and nanosized crystals, it is found that there is no obvious difference in the observed data, which suggests that both PDA−ETCD and PDA−PUDO bulk crystals retain similar crystal structures while crystal size decreases down to micro- and nanoscale.

Acknowledgment. The work at the University of Massachusetts Lowell was supported in part by the Petroleum Research Fund under Grant 40263-AC7. In summers 2005 and 2006, X. Wang was supported by a Faculty Student Collaborative Research Grant. The authors thank M. J. Downey for furnishing X-ray powder diffraction patterns and Professor John Warner for the use of his DSC instrument. The work at the University of Massachusetts Amherst was supported by the U.S. Army Research Office (ARO W911NF-04-1-0329) and the W.M. Keck Electron Microscopy Laboratory.

Supporting Information Available: FTIR spectra of various forms of PDA−ETCD and PDA−PUDO. This material is available free of charge via the Internet at http://pubs.acs.org.

References and Notes

(1) Kasai, H.; Nalwa, H. S.; Oikawa, H.; Okada, S.; Matsuda, H.; Minami, N.; Kakuta, A.; Ono, K.; Mukoh, A.; Nakanishi, H. *Jpn. J. Appl. Phys.* **1992**, *31*, L1132−L1134.

(2) Nakanishi, H.; Kasai, H. In *Photonic and Optoelectronic Polymers*; ACS Symposium Series; Jenekhe, S. A., Wynne, K. J., Eds.; American Chemical Society: Washington, DC 1997, Vol. 672, pp 183−198.

(3) Yang, K.; He, J.-A.; Kumar, J.; Samuelson, L. A.; Oshikiri, T.; Katagi, H.; Kasai, H.; Okada, S. Oikawa, H.; Nakanishi, H. *J. Opt. Soc. Am. B* **2005**, *22*, 6123−6132.

(4) (a) Katagi, H.; Kasai, H.; Okada, S.; Oikawa, H.; Matsuda, H.; Nakanishi, H. *J. Macromol. Sci., Pure Appl. Chem.* **1997**, *A34*, 2013−2024. (b) Nakanishi, H.; Katagi, H. *Supramol. Sci.* **1998**, *5*, 289−295. (c) Oikawa, H.; Oshikiri, T.; Kasai, H.; Okada, S.; Tripathy, S. K.; Nakanishi, H. *Polym. Adv. Technol.* **2000**, *11*, 783−790. (d) Onodera, T.; Oshikiri, T.; Katagi, H.; Kasai, H.; Okada, S.; Oikawa, H.; Terauchi, M.; Terauchi, M.; Tanaka, M.; Nakanishi, H. *J. Cryst. Growth* **2001**, *229*, 586−590. (e) Volkov, V. V.; Asahi, T.; Masuhara, H.; Masuhara, A.; Kasai, H.; Oikawa, H.; Nakanishi, H. *J. Phys. Chem. B* **2004**, *108*, 7674−7680.

(5) Sandman, D. J.; Kim, I.-B.; Njus, J. M.; Lee, D.-C.; Cholli, A. L.; Sahoo, S. *Macromol. Symp.* **2003**, *192*, 99−113.

(6) Eckert, H.; Yesinowski, J. P.; Sandman, D. J.; Velazquez, C. S. *J. Am. Chem. Soc.* **1987**, *109*, 761−768.

(7) Sandman, D. J.; Elman, B. S.; Hamill, G. P.; Velazquez, C. S.; Samuelson, L. A. *Mol. Cryst. Liq. Cryst.* **1986**, *134*, 89−107.

(8) Sandman, D. J. *Trends Polym. Sci.* **1997**, *5*, 71−74.

(9) Wang, X.; Yang, K.; Ye, H.; Wang, Y.; Lee, J. S.; Sandman, D. J. *J. Macromol. Sci., Pure Appl. Chem.* **2006**, *A43*, 1937−1943.

(10) Sandman, D. J.; Samuelson, L. A.; Velasquez, C. S. *Polym. Commun.* **1986**, *27*, 242−243.

(11) Kubel, C.; Martin, D. C. *Philos. Mag. A* **2001**, *81*, 1651−1673.

(12) Chance, R. R.; Baughman, R. H.; Mueller, H.; Eckhardt, C. J. *J. Chem. Phys.* **1977**, *67*, 3616−3618.

(13) Koshihara, S.; Tokura, Y.; Takeda, K.; Koda, T. *Phys. Rev. Lett.* **1992**, *68*, 1148.

(14) (a) Downey, M. J.; Hamill, G. P.; Rubner, M.; Sandman, D. J.; Velazquez, C. S. *Makromol. Chem.* **1988**, *188*, 1199−1205. (b) Tanaka, H.; Gomez, M. A.; Tonelli, A. E.; Lovinger, A. J.; David, D. D.; Thakur, M. *Macromolecules* **1989**, *22*, 2427−2432. (c) Koshihara, S.; Tokura, Y.; Takeda, K.; Koda, T.; Kobayashi, A. *J. Chem. Phys.* **1990**, *92*, 7581−7588.

(15) West, A. R. *Solid State Chemistry and Its Applications*; John Wiley & Sons: Chichester, UK, 1984; Chapter 5, pp 173−175.

(16) Takeda, K.; Koda, T.; Koshihara, S.; Tokura, Y. *Synth. Met.* **1991**, *41*, 231−234.

(17) Hankin, S. H. W.; Downey, M. J.; Sandman, D. J. *Polymer* **1992**, *33*, 5098−5101.

(18) Lee, D.-C.; Sahoo, S. K.; Cholli, A. L.; Sandman, D. J. *Macromolecules* **2002**, *35*, 4347−4355.

MA070820X